Inverse-dynamics model eye movement control by Purkinje cells in the cerebellum

M. Shidara*, K. Kawano*, H. Gomi† & M. Kawato†‡

* Neuroscience Section, Electrotechnical Laboratory, 1-1-4 Umezono, Tsukuba-shi, Ibaraki 305, Japan
† ATR Human Information Processing Research Laboratory, Soraku-gun, Kyoto 619-02, Japan
‡ Laboratory of Parallel Distributed Processing, Research Institute for Electronic Science, Hokkaido University, Sapporo-city, Hokkaido 060, Japan

MANY lines of evidence suggest that the cerebellum is involved in motor control[1]. But what features of these movements are encoded by cerebellar neurons? For slow-tracking eye movements, the activity of Purkinje cells in the ventral paraflocculus of the cerebellum is known to be correlated with eye velocity[2–5] and acceleration[5]. Here we show that the complex temporal pattern of the firing frequency that occurs during the ocular following response elicited by movements of a large visual scene[6–8] can be reconstructed by an inverse-dynamics representation, which uses the position, velocity and acceleration of eye movements. Further analysis reveals that the velocity and acceleration components can provide appropriate dynamic drive signals to ocular motor neurons, whereas the position component often has the wrong polarity. We conclude that these Purkinje cells primarily contribute dynamic command signals.

Figure 1 shows the sample simple spike activity of a Purkinje cell (P cell) in the left ventral paraflocculus of a monkey together with the ocular following response to 65 presentations of a 160 deg s^{-1} downward test ramp of a large random-dot pattern. Responses were aligned with stimulus onset (time 0). From top to bottom, the ensemble average spike response over the 65 trials of this P cell, eye acceleration, velocity and position, and stimulus velocity are shown. The firing rate of this neuron becomes significantly different from the baseline rate 51 ms after the onset of stimulus motion. In the data shown here, the eyes began moving several milliseconds after the onset of the neural responses. To analyse the information represented in the activity of the P cell, a temporal pattern of ensemble average firing frequency of the P cell was reconstructed by the inverse-dynamics representation method[9–11] as follows:

$$f(t-\Delta) = a \cdot e''(t) + b \cdot e'(t) + c \cdot e(t) + d \qquad (1)$$

where $f(t)$, $e''(t)$, $e'(t)$, $e(t)$, Δ are the firing frequency at time t, the eye acceleration, velocity and position at time t, and the

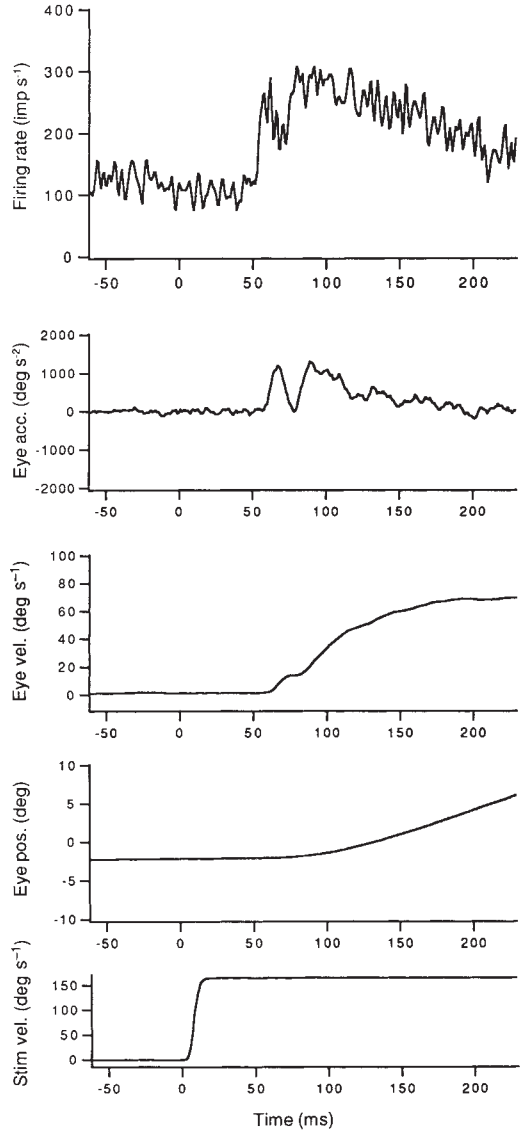

FIG. 1 Simple spike activity of a P cell in the left ventral parafocculus and the ocular following responses to 65 presentations of a 160 deg s^{-1} downward test ramp. Responses are aligned at a stimulus onset (Time 0). From top to bottom: ensemble average firing frequencies, averaged vertical eye acceleration, velocity and position, and averaged stimulus velocity profiles. Upward direction in the figure means downward eye or stimulus movements. All eye-movement data were filtered with a 6-pole Bessel low-pass filter (cut-off, 100 Hz). Latency was 51 ms for unit activity.

METHODS. The animals (*Macaca fuscata*) had been previously trained to fixate a small target spot to obtain a fluid reward. Under Nembutal anaesthesia and aseptic conditions, each monkey was implanted with a cylinder for microelectrode recording, and fitted with a head holder that allowed the head to be fixed in the standard stereotaxic position during the experiments. Scleral search coils were implanted for measuring eye movements[21]. The animals faced a translucent tangent screen (85° × 85° at a distance of 235 mm) on which moving random-dot patterns could be back-projected. The visual stimulus started to move 150 ms after the end of a centering saccade with eight directions at 10–160 deg s^{-1}. Each visual stimulus ramp lasted 250 ms. Voltage signals separately encoding the horizontal and vertical components of eye position, eye velocity, and mirror (stimulus) velocity were digitized to a resolution of 12 bits, sampling at 500 Hz[8]. The acceleration profiles were obtained by digital differentiation of eye velocity profiles after averaging. A time–amplitude window discriminator was used to record spike occurrences with a time resolution of 1 ms.

TABLE 1 Significance of each component in the reconstructed firing frequency

	$P<0.005$	$0.005 \leq P \leq 0.05$	$P>0.05$
Acceleration component	18	1	0
Velocity component	19	0	0
Position component	16	0	3
Bias component	19	0	0

P values of *t*-tests are for the null hypothesis that a coefficient of each component is zero, and indicate the probability that the model fitting is performed well when a particular component is dropped. Numbers denote the number of cells.

time delay between firing frequency and movement, respectively. Four coefficients (a, b, c, d) and the time delay (Δ) were estimated to minimize the squared error between the average and reconstructed firing frequencies. This inverse-dynamics equation looks similar to the forward-dynamics model of the eye plant, which predicts the movement from the motor command, but is very different from and actually opposes it in the direction of information flow[12,13].

If we assume, for simplicity, the final motor neuron command $m(t)$ to be the weighted sum of the firing $f_i(t)$ of the ith P cell weighted by w_i, and the firing $g_j(t)$ of the jth neuron weighted by p_j in another brain region, then we can derive the following second-order forward-dynamics equation with the acceleration, velocity and position coefficients M, B, K[14,15]:

$$M \cdot e''(t) + B \cdot e'(t) + K \cdot e(t) = m(t-\Delta_m) = \sum_{i=1}^{N} w_i \cdot f_i(t-\Delta_i) + \sum_{j=1}^{L} p_j \cdot g_j(t-\Delta_j) \quad (2)$$

This forward-dynamics equation requires that all casual inputs are to the eye plant and can be used only for the final common path[14,16] not for a single P cell: that is, movement cannot be predicted from single P cell firing. But the inverse-dynamics represented in equation (1) can be used for a single P cell if its output contributes to the final motor command. Furthermore, in this inverse-dynamics representation any coefficients (a, b, c) would be negative if activities of other cells or regions compensate for its negative contribution to provide the final and stable motor neuron command: that is, the single P cell firing could be reconstructed from the movement.

The response properties of the P cell whose 160 deg s^{-1} response is shown in Fig. 1 were next studied at five different stimulus velocities (10, 20, 40, 80, 160 deg s^{-1}). Parameter estimation was made for data from all five velocities together. The estimation error was minimal at 8 ms delay. The determination coefficient[17], which is the square of the correlation coefficient (r^2), was 0.84, indicating that the simple linear inverse-dynamics representation can satisfactorily predict complex time courses of P cell firing.

Figure 2*A* shows the superimposed traces of the raw firing frequency (black dotted line) and the reconstructed firing frequency (red line) of the P cell in Fig. 1 using these parameters, together with the contribution of each component of the eye movements to the reconstructed firing frequency. Although the acceleration coefficient (a) was small (0.11 spikes s^{-1} per deg s^{-2}), its component ($a \cdot e''(t)$; purple line) was predominant in the initial phase of the response and the velocity component ($b \cdot e'(t)$; green line) was dominant in most of the rest. In the later phase, the acceleration component decreased and the position ($c \cdot e(t)$; blue line) component increased. The position component, however, was of reversed sign compared with the direction of the movements.

The successful reconstruction of the firing frequency at differ-

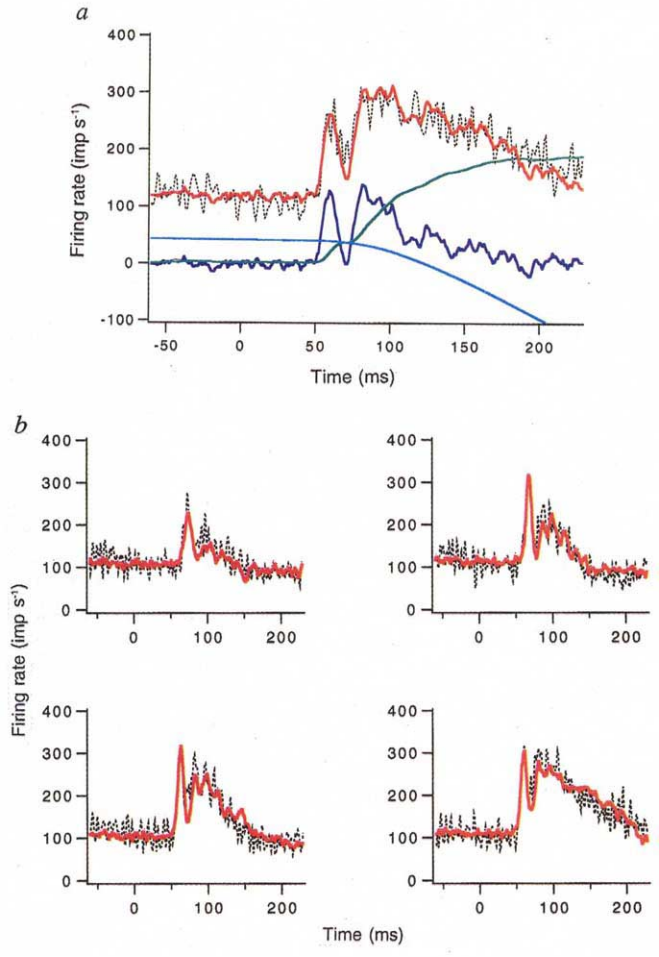

FIG. 2 Reconstruction of temporal pattern of firing frequency of a P cell by inverse-dynamics representation using the position, velocity and acceleration of the eye movements. The temporal pattern of the ensemble average firing frequency of the P cell in Fig. 1 was reconstructed, using the data at stimulus velocities of 10, 20, 40, 80 and 160 deg s^{-1} together. The squared error for model fitting reached minimum at a delay of 8 ms. The determination coefficient was 0.84. The acceleration coefficient was 0.11 spikes s^{-1} per deg s^{-2}, the velocity coefficient was 2.7 spikes s^{-1} per deg s^{-1}, the position coefficient was -20.4 spikes s^{-1} deg^{-1}. For superimposition, eye movement profiles were shifted by the delay time. *A*, Reconstructed firing frequency profile of a P cell superimposed on the raw firing frequency profile, and the reconstructed acceleration, velocity and position components. The stimulus velocity was 160 deg s^{-1}. Reconstructed firing frequency profile (red line), raw firing frequency profile (black dotted line), acceleration component (purple line), velocity component (green line), position component (blue line). *B*, Reconstruction of temporal pattern of firing frequency of the P cell at different stimulus velocities: *a*, 10 deg s^{-1}; *b*, 20 deg s^{-1}; *c*, 40 deg s^{-1}; *d*, 80 deg s^{-1}. Reconstructed firing frequency profile is represented by a red line, and the raw firing frequency profile by a black dotted line.

METHODS. The temporal pattern of ensemble average firing frequency of a P cell was reconstructed as a time series from linear combinations of the eye position, velocity and acceleration after a fixed delay time for the firing frequency, and a bias term. Four coefficients and the time delay were estimated to minimize the squared estimation error. The calculation was done using Mathematica on a Sun Sparc Station.

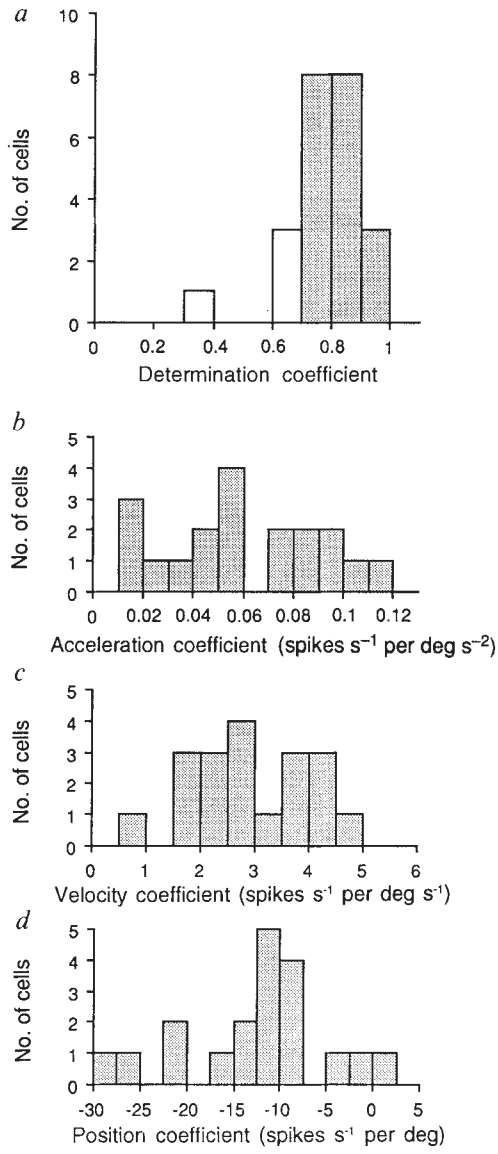

FIG. 3 The distribution of various parameters in model fitting. *a*, Determination coefficients of 23 P cell at the stimulus velocity of 80 or 160 deg s^{-1}. Shaded bars ($n=19$) indicates data whose determination coefficients were more than 0.7. The subsequent statistical analysis was performed on these 19 well-fitted P cells. *b*, Acceleration coefficients of 19 P cells. The mean (±s.d.) was 0.061 (±0.032) spikes s^{-1} per deg s^{-2}. *c*, Velocity coefficients; mean (±s.d.) was 2.9 (±1.0) spikes s^{-1} per deg s^{-1}. *d*, Position coefficients; mean (±s.d.) was −12.6 (±7.8) spikes s^{-1} deg^{-1}.

ent stimulus velocities by a single set of parameters (Fig. 2*A*: 160 deg s^{-1}; Fig. 2*B*: *a*, 10 deg s^{-1}; *b*, 20 deg s^{-1}; *c*, 40 deg s^{-1}; *d*, 80 deg s^{-1}) indicates the generality of the model.

We studied 43 P cells in the left ventral paraflocculus of two monkeys at a stimulus velocity of 80 or 160 deg s^{-1} (ref. 8). Of these P cells, the same analysis was executed on 23 P cells whose activities could be recorded during the 252 ms after stimulus onset on more than 25 trials without contamination of saccades. The determination coefficient was more than 0.7 in 19 cases (Fig. 3*a*). The parameters of the 19 well fitted P cells were analysed statistically. The mean delay was 7.1 ms (±2.8 ms s.d.), which was near the latency of electrical-stimulation-evoked eye movements[8]. This satisfies a basic prerequisite for the firing frequency to represent the motor command. The distribution of each coefficient is shown in Fig. 3*b*–*d*. The acceleration coefficient had a value of 0.061 ± 0.032 spikes s^{-1} per deg s^{-2} (mean ± s.d.). The velocity coefficient was 2.9 ± 1.0 spikes s^{-1} per deg s^{-1} (mean ± s.d.). The position coefficient was −12.6 ± 7.8 spikes s^{-1} deg^{-1} (mean ± s.d.). The significance of each component was tested by *t*-tests for the null hypothesis that each coefficient is zero; the results are shown in Table 1. The P values for each coefficient were less than 0.005 in most cases, indicating that all components were significant in contributing to the firing frequency. Further, we tested whether the firing frequency could be well fitted by dropping any of the components. The results were that the determination coefficients (r^2) for the reduced models were significantly smaller (mean was 0.73, 0.55 or 0.71 for dropping $a \cdot e''$, $b \cdot e'$ or $c \cdot e$, respectively) than the three component model (mean 0.82), indicating that all the components were necessary to represent the firing frequency.

To compare each component pertaining to P cells with its motor neuron equivalent we examined the ratios of the coefficients. The mean ratio of acceleration coefficient to velocity coefficient (b/a) of the P cells was 72.1 (±72.4 s.d.), which was close to that of motor neurons at 67.4 (ref. 15). On the other hand, whereas the mean ratio of acceleration coefficient to position coefficient ($c/a = -294.5$ (±261.8 s.d.)) of P cells was comparable in size to that of motor neurons (344.8; ref. 15), it was different and had a reversed sign, suggesting that there are other inputs to motor neurons that effectively cancel these inappropriate position signals from the ventral paraflocculus, with the net effect that these P cells contribute to the dynamic (velocity and acceleration) rather than the static (position) control of eye movements. Although the mean ratio of acceleration and velocity coefficients of P cells is close to that of motor neurons, the mean ratio of visual mossy fibre inputs to P cells is only ~50% (unpublished observations): that is, although the output from P cells may constitute the dynamic part of the final motor command, their inputs cannot. The inverse-dynamics problem could be solved at multiple sites in the brain, but our results support the hypothesis that the cerebellum may represent a major site for inverse-dynamics modelling of controlled movements[13,18 20]. This computational hypothesis could be rigorously tested by applying our analysis to different sites in the brain whose activities are related to the ocular following response. □

Received 29 March; accepted 17 June 1993.

1. Ito, M. *The Cerebellum and Neural Control* (Raven, New York, 1984).
2. Miles, F. A. & Fuller, J. H. *Science* **189,** 1000–1002 (1975).
3. Lisberger, S. G. & Fuchs, A. F. *J. Neurophysiol.* **41,** 733–763 (1978).
4. Miles, F. A., Fuller, J. H., Braitman, D. J. & Dow, B. M. *J. Neurophysiol.* **43,** 1437–1476 (1980).
5. Stone, L. S. & Lisberger, S. G. *J. Neurophysiol.* **63,** 1241–1261 (1990).
6. Miles, F. A., Kawano, K. & Optican, L. M. *J. Neurophysiol.* **56,** 1321–1354 (1986).
7. Kawano, K., Shidara, M. & Yamane, S. *J. Neurophysiol.* **67,** 680–703 (1992).
8. Shidara, M. & Kawano, K. *Expl Brain Res.* **93,** 185–195 (1993).
9. Hollerbach, J. M. in *Robot Motion* (eds Brady, M., Hollerbach, J. M., Johnson, T. L., Lozano-Perez, T. & Mason, M. T.) (MIT Press, Cambridge, Massachusetts, 1982).
10. Kawato, M., Furukawa, K. & Suzuki, R. *Biol. Cybern.* **57,** 169–185 (1987).
11. Atkeson, C. G. *A. Rev. Neurosci.* **12,** 157–183 (1989).
12. Barto, A. G. in *Neural Networks for Control* (eds Miller, T., Sutton, R. & Werbos, P.) 5–58, (MIT Press, Cambridge, Massachusetts, 1990).
13. Kawato, M. & Gomi, H. *Trends Neurosci.* **15,** 445–453 (1992).
14. Robinson, D. A. in *Handbook of Physiology* Sect. 1, Vol. II, 1275–1320 (ed Brooks, V. B.) (Am. Physiol. Soc., Waverly, Baltimore, 1960).
15. Keller, E. L. *Vision Res.* **13,** 1565–1575 (1973).
16. Bethier, N. E., Barto, A. G. & Moore, J. E. *Biol. Cybern.* **65,** 99–105 (1991).
17. Walpole, R. E. & Meyers, R. H. *Probability and Statistics for Engineers and Scientists* (Macmillan, New York, 1978).
18. Kawato, M. & Gomi, H. *Biol. Cybern.* **68,** 95–103 (1992).
19. Gomi, H. & Kawato, H. *Biol. Cybern.* **68,** 105–114 (1992).
20. Kawato, M. & Gomi, H. *Trends Neurosci.* **16,** 177–178 (1993).
21. Judge, S. J., Richmond, B. J. & Chu, F. C. *Vision Res.* **20,** 535–538 (1980).

ACKNOWLEDGEMENTS. We thank M. P. Young, F. A. Miles and F. E. Pollick for improving the manuscript. This work was partly supported by grants to K.K. and M.K. from the Human Frontier Science Program.